GEUS Bulletin | Geological Survey of Denmark and Greenland

DATA ARTICLE | SHORT

A whole-rock data set for the Skaergaard intrusion, East Greenland

Christian Tegner*[1], Lars Peter Salmonsen[2], Marian B. Holness[3], Charles E. Lesher[1], Madeleine C. S. Humphreys[3,4], Peter Thy[5], Troels F. D. Nielsen[6]

[1]Department of Geoscience, Aarhus University, Aarhus, Denmark; [2]Rambøll, Aarhus, Denmark; [3]Department of Earth Sciences, University of Cambridge, Cambridge, UK; [4]Department of Earth Sciences, Durham University, Durham, UK; [5]Department of Earth and Planetary Sciences, University of California, Davis, USA; [6]Department of Mapping and Mineral Resources, Geological Survey of Denmark and Greenland, Copenhagen, Denmark

Abstract

We report a compilation of new and published whole-rock major and trace element analyses for 646 samples of the Skaergaard intrusion, East Greenland. The samples were collected in 14 stratigraphic profiles either from accessible and well-exposed surface areas or from drill core, and they cover most regions of the intrusion. This includes the Layered Series, the Upper Border Series, the Marginal Border Series and the Sandwich Horizon. The geochemical data were obtained by a combination of X-ray fluorescence and inductively coupled plasma mass spectrometry. This data set can, for example, be used to constrain processes of igneous differentiation and ore formation.

Tabular abstract

Geographical coverage	The Skaergaard intrusion occupies a *c.* 11 × 8 km outcrop area of layered gabbroic rocks at Uttentals Sund, Kangerlussuaq area, East Greenland. Located at *c.* 68°9 'N and 31°41' W.
Temporal coverage	Palaeogene (*c.* 56.0 Ma)
Subject(s)	Cosmochemistry and geochronology, economic geology, geochemistry, igneous rocks and processes
Data format(s)	Major and trace element compositions reported in an Excel spreadsheet.
Sample collection & analysis	Samples (*n* = 646) taken from surface outcrops and drill cores were analysed by X-ray fluorescence and inductively coupled plasma mass spectrometry (ICP-MS). The samples are stored and curated at: Aarhus University (surface samples from the Layered Series and Upper Border Series); Geological Survey of Denmark and Greenland (surface samples from the Layered Series); Natural History Museum of Denmark, University of Copenhagen (drill core samples) and the Harker Collection of the Sedgwick Museum, University of Cambridge (Cambridge 1966 drill core and surface samples of the Marginal Border Series).
Parameters	Major and trace element whole-rock compositions.
Related publications:	Tegner 1997; Tegner *et al.* 2009; Salmonsen & Tegner 2013; Holness *et al.* 2015, 2017, 2022; Thy *et al.* in press.
Potential application(s) for these data	This data set can, for example, be used to constrain processes of igneous differentiation and ore formation.

Data collection

To examine the petrology and ore bodies of the Skaergaard Intrusion, East Greenland, we have collected hundreds of samples during six field expeditions between 1993 and 2017. In addition, we have collected samples from drill core material housed at the Natural History Museum of Denmark

***Correspondence:** *christian.tegner@geo.au.dk*
Received: 05 Apr 2022
Revised: 01 Mar 2023
Accepted: 13 Apr 2023
Published: 15 June 2023

Keywords: Skaergaard intrusion, layered mafic intrusion, bulk-rock geochemical data, X-ray fluorescence (XRF), inductively coupled plasma mass spectrometry (ICP-MS)

Abbreviations
a.s.l.: above sea level
F: mass fraction of melt remaining in the chamber
GEUS: Geological Survey of Denmark and Greenland.
HZ: Hidden Zone
ICP-MS: inductively coupled plasma mass spectrometry
LOI: mass lost on ignition
LS: Layered Series
LZ: Lower Zone
MZ: Middle Zone
s.d.: standard deviation
SH: Sandwich Horizon
UZ: Upper Zone
XRF: X-ray fluorescence

Edited by: Kerstin Saalmann (Geological Survey of Norway)

Reviewed by: Rais Latypov (University of Witwatersrand, South Africa), Howard Naslund (Binghamton University, USA)

Funding: See page 7

Competing interests: See page 7

Additional files: See page 7

(University of Copenhagen) and the Harker Collection of the Sedgwick Museum (University of Cambridge). Here, we report a compilation of 646 whole-rock analyses for these samples attached as one Excel spreadsheet (Supplementary Data File 1). All samples were analysed by X-ray fluorescence (XRF); most of these data (n = 409) were published in Tegner (1997), Tegner *et al.* (2009), Salmonsen & Tegner (2013), Holness *et al.* (2015, 2022) and Thy *et al.* (in press). The remaining analyses (n = 237) are reported here for the first time apart from P_2O_5 data (n = 167), which were reported in Holness *et al.* (2017). A subset of 271 samples were analysed by inductively coupled plasma mass spectrometry (ICP-MS). About half of these (n = 130) were published in Tegner *et al.* (2009) and Thy *et al.* (in press); the remaining analyses (n = 141) are reported here for the first time. The analysed samples mainly represent mafic cumulate rocks (n = 623) but also include gabbropegmatite and granophyric pods and layers (n = 23). Details of subsets of the present bulk-rock data set have been described and discussed in a number of publications (e.g. Tegner 1997; Tegner *et al.* 2009; Thy *et al.* 2009, in press; Tegner & Cawthorn 2010; McKenzie 2011; Salmonsen & Tegner 2013; Namur *et al.* 2013, 2014; Holness *et al.* 2015, 2017, 2022; Nielsen *et al.* 2015; Keays & Tegner 2016; Pedersen *et al.* 2021).

The samples were collected in 14 stratigraphic profiles as shown on the geological map (Fig. 1), in a schematic cross-section (Fig. 2), listed in Table 1 and described in detail in Supplementary Data File 2. The sample sections thus cover the known stratigraphy and rock units reported in the Layered Series (LS: including Hidden Zone, HZ; Lower Zone a, LZa; Lower Zone b, LZb; Lower Zone c, LZc; Middle Zone, MZ; Upper Zone a; UZa; Upper Zone b, UZb; Upper Zone C, UZc), the Marginal Border Series (MBS: including Lower Zone a*, LZa*; Lower Zone b*, LZb*; Lower Zone c*, LZc*; Middle Zone*, MZ*; Upper Zone a*; UZa*; Upper Zone b*, UZb*; Upper Zone C*, UZc*), the Upper Border Series (UBS: including Lower Zone a´, LZa´; Lower Zone b´, LZb´; Lower Zone c´, LZc´; Middle Zone´, MZ´; Upper Zone a´; UZa´; Upper Zone b´, UZb´; Upper Zone C´, UZc´), and the Sandwich Horizon (SH). This zonal subdivision is outlined in Figs 1 and 2. A field photograph (Fig. 3) shows an example of layered rocks (Layered Series). Further selected outcrops are shown in Fig. S1 (Supplementary Data File 2). Previous work has shown that the intrusion represents the result of prolonged, uninterrupted differentiation of a tholeiitic magma (Wager & Deer 1939; Wager & Brown 1968; Naslund 1984; Hoover 1989; McBirney 1996; Irvine *et al.* 1998). Palladium and gold mineralisations have been identified in the LS (Andersen *et al.* 1998; Nielsen *et al.* 2015). A key point is that the LS, MBS and UBS appear to represent continuous and synchronous crystallisation on the floor, margins and roof and SH the products of the most evolved, last drops of magma in the interior of the intrusion. These rocks, therefore, allow evaluation of the processes resulting in igneous differentiation and ore formation in opposite positions relative to gravity (e.g. McBirney 1995).

Sample profiles

The stratigraphic profiles (n = 14) are summarised in Table 1 and illustrated in Figs 1 and 2. The profiles cover most regions of the intrusion and were collected either from accessible and well exposed surface areas or from drill core. The details of the sample profiles are described in Supplementary Data File 2.

Sampling strategy

The sampling was directed to obtain mainly average rock compositions in systematic stratigraphic sections. Additional samples of outcrop features such as gabbropegmatites, subzone boundaries and layered structures were also included, for example, the 'wavy pyroxene rocks' and colloform banding of the MBS (Humphreys & Holness 2010; Namur *et al.* 2013). The sample positions were recorded by GPS and altimeter readings (Supplementary Data File 1). For LS and UBS, the stratigraphic thicknesses were calculated relative to the local strike and dip of layering as described previously (Tegner *et al.* 2009; Salmonsen & Tegner 2013) and are listed in Supplementary Data File 1. Within the limitations of outcrops, we aimed to sample at regular stratigraphic intervals. For LS and UBS, the average stratigraphic interval was 12 ± 13 m (1 s.d.). For MBS, the lateral distance from the contact is recorded and the average spacing between samples was 18 ± 6 m (1 s.d.; Holness *et al.* 2022).

Calculation of fraction of melt remaining (*F*)

The box-like appearance of the intrusion with onion-ring distribution of zones and subzones (Fig. 2) implies that stratigraphic thickness, and mass proportions are not proportional (Nielsen 2004). Based on mass proportions estimated for each subzone in the floor, wall and roof series (Nielsen 2004), the mass fraction of melt remaining in the chamber, F, can be estimated for subzone boundaries. For the 'reference profile' of LS, a second-order polynomial was fitted to subzone boundaries to relate F to stratigraphic height (H) and given below as equation 1 (Tegner *et al.* 2009):

$$F = 1.091 \times 10^{-7}H^2 - 5.9064 \times 10^{-4}H + 0.7678 \qquad (1)$$

The F values for the 90-10 and 90-23 drill core samples were also estimated using equation 1 and tied to the 'reference profile' at the H of the UZa/b boundary

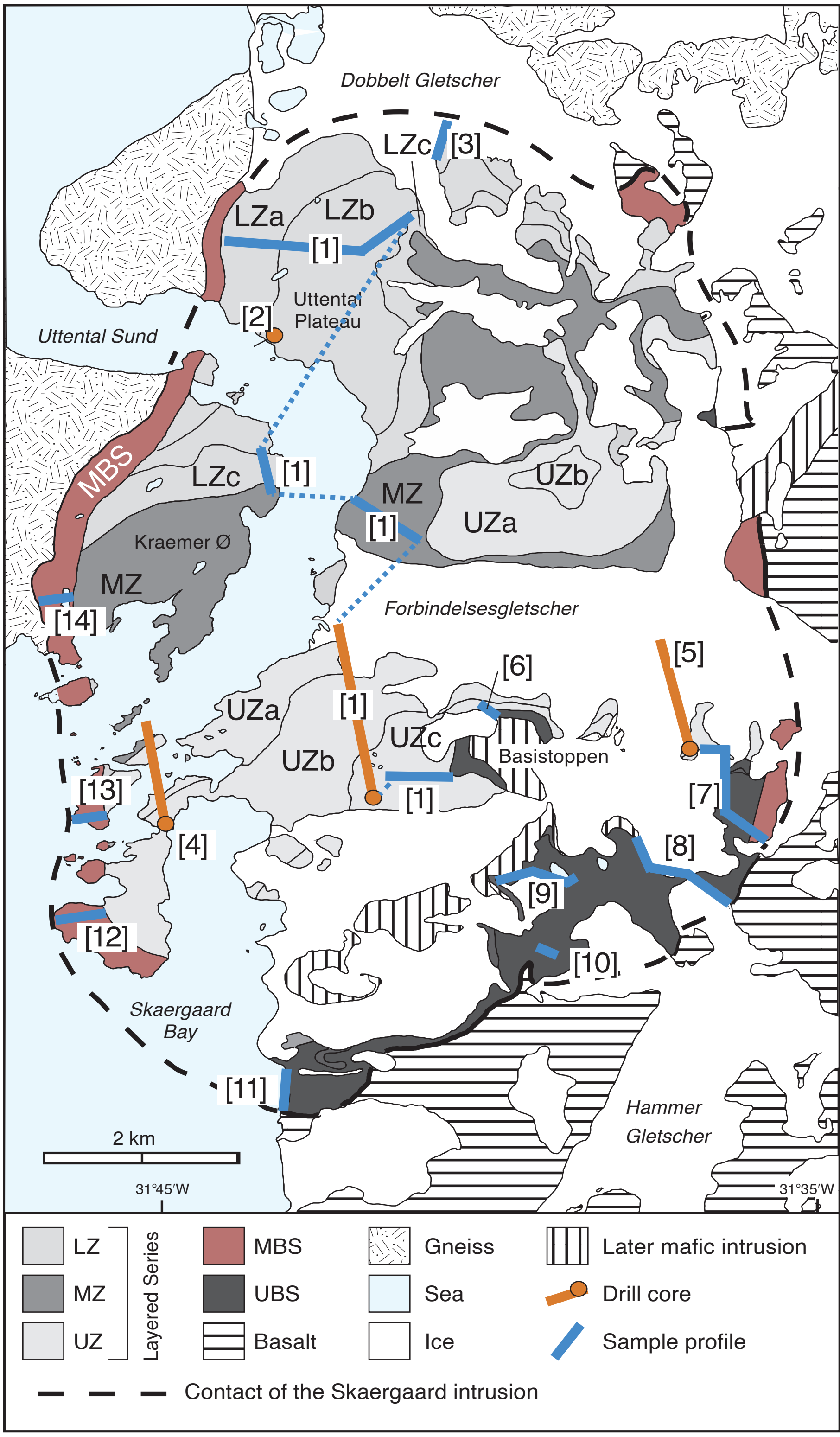

Fig. 1 Geological map of the Skaergaard intrusion and adjacent host rocks. The rocks that solidified at the floor (Layered Series composed of Lower Zone, **LZ**, Middle Zone, **MZ**, and Upper Zone, **UZ**), walls (Marginal Border Series, **MBS**) and roof (Upper Border Series, **UBS**) are shown. Also shown are the approximate locations of 14 sample profiles (surface samples and drill cores) that are studied here. The sample profiles are numbered 1 to 14 and listed in Table 1. Further subzone abbreviations are in the text. Modified from McBirney (1989).

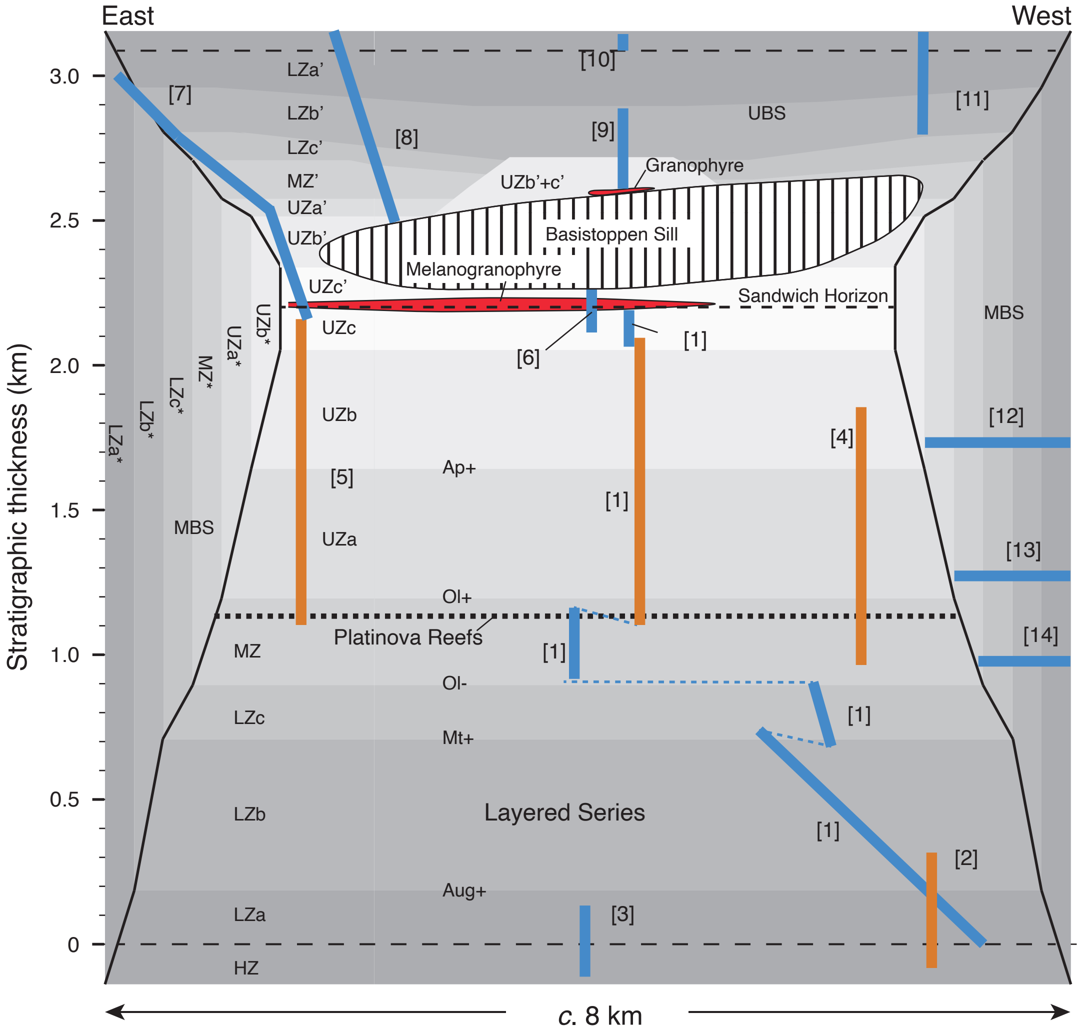

Fig. 2 Schematic cross-section of the Skaergaard intrusion showing the distribution of rocks that solidified at the floor (Layered Series), the walls (Marginal Border Series, **MBS**) and the roof (Upper Border Series, **UBS**). Also shown are the approximate locations of 14 sample profiles (surface samples: **blue lines**, drill cores: **orange lines**) that are studied here. The sample profiles are also shown on the map in Fig. 1 and numbered 1 to 14 as listed in Table 1. The floor, wall and roof sequences are divided into subzones (HZ–UZc) depending on the appearance and disappearance of primary (cumulus) crystal phases as marked on the subzone boundaries. Abbreviations: **HZ**: Hidden Zone. **LZ**: Lower Zone. **MZ**: Middle Zone. **UZ**: Upper Zone. **SH**: Sandwich Horizon. Further subzone abbreviations and nomenclature are in the text. Modified from McBirney (2002) and Nielsen (2004).

(1615 m). Similarly, the *F* values for the samples of the Cambridge Core were estimated with equation 1, setting *H* to zero at the LZa/HZ boundary (Holness *et al.* 2015). For UBS, *F* values of subzone boundaries were fixed to the same values as for LS, and *F* values of samples were related to stratigraphic height by linear interpolation (Salmonsen & Tegner 2013). Similarly for MBS, the *F* values at subzone boundaries were assumed equal to those of LS, and the *F* values of the samples were related to the distance between subzone boundaries by linear interpolation. Finally, in the sections crossing the SH, we assigned an *F* value of zero to the sample with the lowest MgO content (≤0.02 wt%). The estimated *F* values are reported in Supplementary Data File 1.

Analytical methods

All samples were collected, prepared and analysed in the same way. From surface outcrops, we collected samples weighing 1–4 kg and avoiding alteration veins. The samples were trimmed for surface weathering by sawing, and an aliquot (100–400 g) was crushed to small aggregates (<2 cm) in a hydraulic steel press. This was followed by splitting, pre-contamination of a corundum shatterbox, cleaning and finally powdering of *c.* 30 g. The drill core material was prepared in the same way with one exception. The powders of drill core 90-22 (n = 51) were prepared using a steel jaw crusher and a tungsten-carbide shatterbox. All samples were prepared at Aarhus University as described in Tegner *et al.* (2009).

Table 1 Overview of samples and sample profiles

Sample profile		Rock series	Subzones	No. of samples	No. of samples	No. of samples	No. of samples	Reference
Name	No. [b]			Total	Cumulate	Melanogranophyre	Gabbropegmatite	
Reference profile [a]	[1]	Layered Series	LZa, LZb, LZc, MZ, UZa, UZb, UZc	138	135	2	1	Tegner (1997); Tegner *et al.* (2009); Thy *et al.* (in press)
Cambridge drill core	[2]	Layered Series	HZ, LZa	121	121			Holness *et al.* (2015)
Dobbelt Gletscher	[3]	Layered Series	HZ, LZa	8	8			This study
90-10 drill core	[4]	Layered Series	MZ, UZa, UZb	81	81			This study
90-23 drill core	[5]	Layered Series	UZa, UZb, UZc	87	87			This study
NW Basistoppen	[6]	Layered Series/Upper Border Series	UZc, SH, UZc´	21	12	9		This study
Kilen	[7]	Upper Border Series/ Layered Series	HZ´, LZa´, LZb´, LZc´, MZ´, UZa´, UZb´, UZc´, SH; UZc	33	26	6	1	Salmonsen & Tegner (2013)
Hammer Pass	[8]	Upper Border Series	HZ´, LZa´, LZb´, LZc´, MZ´, UZa´	25	25			Salmonsen & Tegner (2013)
Brødretoppen	[9]	Upper Border Series	HZ´, LZa´, LZb´, LZc´, MZ´, UZa´, UZb´, UZc´, SH	37	34	3		Salmonsen & Tegner (2013)
Sydtoppen	[10]	Upper Border Series	HZ´	11	11			Salmonsen & Tegner (2013)
Skaergaard Bay	[11]	Upper Border Series	HZ´, LZa´, LZb´	15	15			This study
Skaergaard Peninsula	[12]	Marginal Border Series	LZa*, LZb*, LZc*, MZ*, UZa*, UZb*	33	33			Holness *et al.* (2022)
Ivnarmiut Island	[13]	Marginal Border Series	LZa*, LZb*, MZ*	17	17			Holness *et al.* (2022)
Kraemer Ø	[14]	Marginal Border Series	LZa*, LZb*	19	19			Holness *et al.* (2022)
Total no. of samples				646	624	20	2	

[a]Reference profile consists of surface samples from Uttental Plateau, Kraemer Ø, Pukugagryggen/Forbindelsesgletscher, West Basistoppen, and drill core 90-22. [b]Numbers labelled in Fig. 1.
LZ: Lower Zone. MZ: Middle Zone. UZ: Upper Zone. HZ: Hidden Zone. SH: Sandwich Horizon.

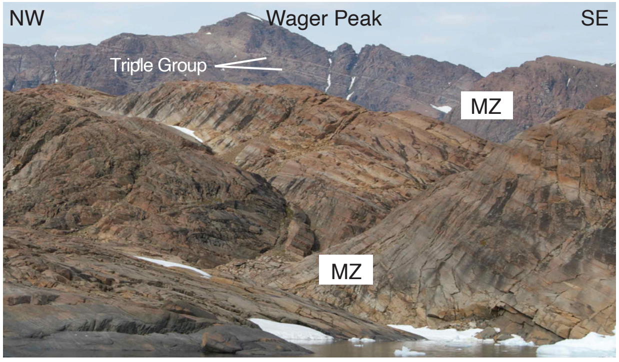

Fig. 3 Field photo showing the northwards view from Kraemer Ø. Metre-scale modal layering occurs in the Middle Zone (**MZ**) (foreground, lower two-thirds) and in the background where the Triple Group can be seen on Wager Peak (*c*. 1200 m a.s.l.).

The major and trace element data were obtained by a combination of XRF at Aarhus University and ICP-MS at the University of California, Davis and AcmeLabs as described in Tegner *et al*. (2009), Thy *et al.* (in press) and Tegner *et al.* (2019), respectively. Concentrations of FeO were determined by titration with potassium dichromate. The mass lost on ignition (LOI) was determined by heating the powder in air in a muffle furnace at 950°C for 3 h. The values obtained for certified reference materials, BHVO-1 and BIR-1, are reported in Supplementary Data File 3. XRF analyses of BHVO-1 and BIR-1 (n = 53–63) demonstrate that the relative variation of repeated analyses is less than 4.5% (1 s.d./average value) for most major element oxides. However, in BIR-1, the relative variation is higher (14%) for K_2O, which has a relatively low concentration (0.027 wt%; Jochum *et al.* 2016). For the trace elements measured by XRF, the relative variation of the transition metals (V, Cr, Ni, Cu, Zn) and Sr are within 5%. In BHVO-1, the relative variation is moderate for Rb, Y, Zr, Nb and Ba (4–12%) and higher for Ce (20%). In BIR-1, which is depleted in these elements relative to BHVO-1 (Jochum *et al.* 2016), the relative variation of repeat analyses is somewhat higher for Rb, Y, Zr and Nb and Pb (7–28%) and much higher for Ba and Ce. The accuracy or relative deviation from the preferred values for BHVO-1 is within 11% for all oxides and trace elements. Similar values were obtained for the accuracy of BIR-1, except for Rb, Nb and Ce, which have sub-ppm preferred values.

In conclusion, the XRF data can generally be viewed as accurate down to a few ppm. Repeat ICP-MS analyses of standards at AcmeLab (n = 14) and University of California (n = 6) deviate less than 7 and 18%, respectively, from the preferred values for all trace elements reported in this study (Supplementary Data File 3).

Data description and main features

The bulk compositions of cumulate rocks, such as those reported here, represent a mix of accumulated

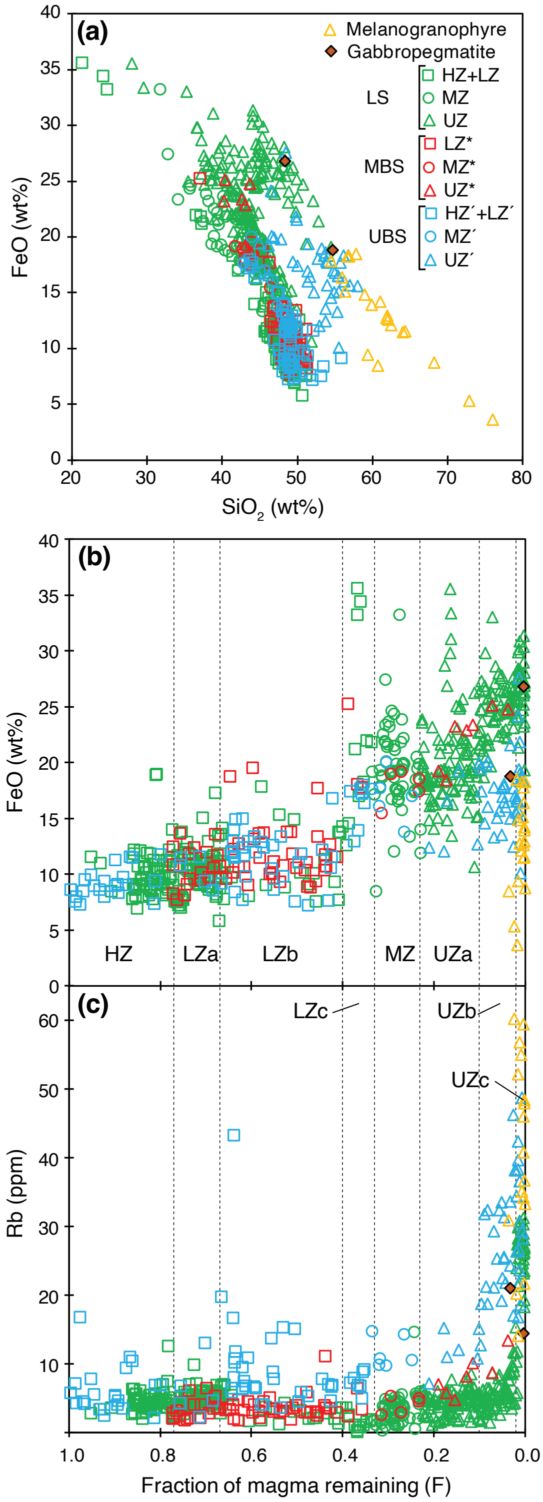

Fig. 4 Example compositional data available in the data set. **a**: Whole-rock FeO^{total} versus SiO_2 (wt%) for the Skaergaard intrusion. One outlier at 17 wt% SiO_2 and 50 wt% FeO is not shown. **b, c**: Stratigraphic variations in whole-rock FeO^{total} and Rb contents. Data from Supplementary Data File 1.

liquidus crystals (cumulus) and interstitial material (intercumulus) derived from crystallisation of interstitial melt (Wager *et al.* 1960; Irvine 1982). The present data set thus tracks changes in the compositions and proportions of minerals and trapped melt during solidification of the Skaergaard magma chamber. Importantly, the bulk-rock compositions do not directly represent liquid compositions. The data set can therefore be used to evaluate igneous processes during crystallisation and ore formation. Figure 4a, for example, shows that bulk-rock FeO^{total} and SiO_2 vary considerably and display a negative correlation. These two oxides also show systematic variations between zones (HZ, LZ, MZ, UZ). The compositions generally overlap between LS, MBS and UBS rocks although the most FeO-rich rocks occur in LS. In the UZ equivalents, the UBS rocks are enriched in SiO_2 relative to LS and MBS rocks. Not surprisingly, the highest SiO_2 and the lowest FeO values are seen for granophyres *sensu lato*. Figure 4 also shows two examples of stratigraphic variations plotted against the calculated fraction of melt remaining (*F*). In Fig. 4b, FeO generally increases from LZ to UZ equivalents and displays a marked increase across the LZb/LZc boundary, reflecting accumulation of magnetite and ilmenite. In the lower and middle part of the stratigraphy (HZ–UZa), the FeO contents are comparable in the floor, wall and roof rocks. However, in UZb' and UZc' of the roof (UBS), FeO is markedly lower compared to LS and MBS rocks. Figure 4c shows the stratigraphic trends of the incompatible element Rb. In the lower and middle parts (HZ–UZa), the trends are relatively flat and display comparable values in rocks from LS and MBS, while higher values are found in UBS rocks. Closer to SH (UZb and UZc equivalents), Rb increases exponentially in the cumulate rocks and shows the highest values in the melanogranophyres. The compiled whole-rock data set can, for example, be used to constrain processes of igneous differentiation and ore formation.

Acknowledgements

We are grateful to the Danish Lithosphere Centre for supporting field work in 2000. Platina Resources were accommodating during the 2008 and 2011 field seasons. The Geological Survey of Denmark and Greenland (GEUS) helped with field logistics in 2017. Platinova Resources Ltd. are thanked for access to drill core material. We thank C. Kent Brooks for inspiring this project. We are indebted to Jakob K. Keiding for help with field work, sample preparation and discussion. We also enjoyed assistance and company in the field from Jens C.Ø. Andersen, Olivier Namur, Anja K.M. Fonseca and Joel A. Simpson. Sidsel Grundvig, Ingrid Aaes and Jette Villesen, Aarhus University, are thanked for help with sample preparation and X-ray fluorescence analyses. We thank two reviewers, Rais Latypov and Howard Naslund, as well as Kerstin Saalmann for careful editorial handling.

Additional information

Funding statement

This work was supported by funding from Danish National Science Research Council (CT, TFDN), the Danish National Research Foundation (TFDN, CEL, CT), the Carlsberg foundation (CT), Aarhus University (CT, LPS), the UK Natural Environment Research Council (MBH, MCSH), the US National Science Foundation under Grant Number NSF-EAR-0208075 (CEL), the UK Royal Society International Joint Project (MBH, CT).

Author contributions

CT: Conceptualisation, Data curation, Funding acquisition, Investigation, Methodology, Supervision, Visualisation, Writing – original draft.
LPS: Investigation, Methodology, Writing – review and editing.
MBH: Conceptualisation, Data curation, Funding acquisition, Investigation, Methodology, Writing – review and editing.
CEL: Investigation, Conceptualisation, Funding acquisition, Methodology, Writing – review and editing.
MCSH: Investigation, Methodology, Writing – review and editing.
PT: Investigation, Methodology, Writing – review and editing.
TFDN: Investigation, Conceptualisation, Funding acquisition, Methodology, Writing – review and editing.

Competing interests

The authors declare no competing interests.

Additional files

Three additional files, including the data set, a description of sample profiles and analytical precision and uncertainty are available at *https://doi.org/10.22008/FK2/HOWW6F*.

References

Andersen, J.C.Ø., Rasmussen, H., Nielsen, T.F.D. & Rønsbo, J.C. 1998: The Triple Group and the Platinova gold and palladium reefs in the Skaergaard Intrusion: stratigraphic and petrographic relations. Economic Geology **93**, 488–509. *https://doi.org/10.2113/gsecongeo.93.4.488*

Holness, M.B., Humphreys, M.C.S., Namur, O., Andersen, J.C.Ø., Tegner, C. & Nielsen, T.F.D. 2022: Crystal mush growth and collapse on a steep wall: the Marginal Border Series of the Skaergaard Intrusion, East Greenland. Journal of Petrology **63**, 1–21. *https://doi.org/10.1093/petrology/egab100*

Holness, M.B., Tegner, C., Namur, O. & Pilbeam, L. 2015: The earliest history of the Skaergaard magma chamber: a textural and geochemical study of the Cambridge drill core. Journal of Petrology **56**, 1199–1227. *https://doi.org/10.1093/petrology/egv034*

Holness, M.B., Tegner, C., Nielsen, T.F.D. & Charlier, B. 2017: The thickness of the mushy layer on the floor of the Skaergaard magma chamber at apatite saturation. Journal of Petrology **58**, 909–932. *https://doi.org/10.1093/petrology/egx040*

Hoover, J.D. 1989: Petrology of the Marginal Border Series of the Skaergaard Intrusion. Journal of Petrology **30**, 399–439. *https://doi.org/10.1093/petrology/30.2.399*

Humphreys, M.C.S. & Holness, M.B. 2010: Melt-rich segregations in the Skaergaard Marginal Border Series: tearing of a vertical silicate mush. Lithos **119**, 181–192. *https://doi.org/10.1016/j.lithos.2010.06.006*

Irvine, T.N. 1982: Terminology for layered intrusions. Journal of Petrology **23**, 127–162. *https://doi.org/10.1093/petrology/23.2.127-a*

Irvine, T.N., Andersen, J.C.Ø. & Brooks, C.K. 1998: Included blocks (and blocks within blocks) in the Skaergaard Intrusion: geological relations and the origins of rhythmic modally graded layers. Geological Society of America Bulletin **110**, 1398–1447. *https://doi.org/10.1130/0016-7606(1998)110<1398:IBABWB>2.3.CO;2*

Jochum, K.P., Weis, U., Schwager, B., Stoll, B., Wilson, S.A., Haug, G.H., Andreae, M.O. & Enzwiler, J. 2016: Reference values following ISO guidelines for frequently requested rock reference materials. Geostandards and Geoanalytical Research **40**, 333–350. *https://doi.org/10.1111/j.1751-908X.2015.00392.x*

Keays, R.R. & Tegner, C. 2016: Magma chamber processes in the formation of the low-sulphide magmatic Au-PGE mineralization of the Platinova Reef in the Skaergaard intrusion, East Greenland. Journal of Petrology **56**(12), 2319–2339. *https://doi.org/10.1093/petrology/egv075*

McBirney, A.R. 1989: Geological map of the Skaergaard Intrusion, East Greenland, 1:20 000. Department of Geology, University of Oregon, Eugene, Oregon, USA.

McBirney, A.R. 1995: Mechanisms of differentiation in the Skaergaard intrusion. Journal of the Geological Society, London, **152**, 421–435. *https://doi.org/10.1144/gsjgs.152.3.0421*

McBirney, A.R. 1996: The Skaergaard intrusion. In: Cawthorn, R.G. (ed.): Layered intrusions. Pp. 147–180. Amsterdam: Elsevier. *https://doi.org/10.1016/S0167-2894(96)80007-8*

McBirney, A.R. 2002: The Skaergaard Layered Series. Part VI. Excluded trace elements. Journal of Petrology **43**, 535–556. *https://doi.org/10.1093/petrology/43.3.535*

McKenzie, D. 2011: Compaction and crystallization in Magma chambers: towards a model of the Skaergaard intrusion. Journal of Petrology **52**(5), 905–930. *https://doi.org/10.1093/petrology/egr009*

Namur, O., Humphreys, M.C.S. & Holness, M.B. 2013: Lateral reactive infiltration in a vertical gabbroic crystal mush, Skaergaard Intrusion, East Greenland. Journal of Petrology **54**, 985–1016. *https://doi.org/10.1093/petrology/egt003*

Namur, O., Humphreys, M.C.S. & Holness, M.B. 2014: Crystallisation of interstitial liquid and latent heat buffering in solidifying gabbros: Skaergaard Intrusion, Greenland. Journal of Petrology **55**, 1389–1427. *https://doi.org/10.1093/petrology/egu028*

Naslund, H.R. 1984: Petrology of the Upper Border Series of the Skaergaard Intrusion. Journal of Petrology **25**, 185–212. *https://doi.org/10.1093/petrology/25.1.185*

Nielsen, T.F.D. 2004: The shape and volume of the Skaergaard Intrusion, Greenland: implications for mass balance and bulk composition. Journal of Petrology **45**, 507–530. *https://doi.org/10.1093/petrology/egg092*

Nielsen, T.F.D., Andersen, J.C.Ø., Holness, M.B., Keiding, J.K., Rudashevsky, N.S., Rudashevsky, V.N., Salmonsen, L.P., Tegner, C. & Veksler, I.V. 2015: The Skaergaard PGE and gold deposit: the result of *in situ* fractionation, sulphide saturation, and magma chamber scale precious metal redistribution by immiscible Fe-rich melt. Journal of Petrology **56**, 1643–1976. *https://doi.org/10.1093/petrology/egv049*

Pedersen, J.M., Ulrich, T., Whitehouse, M.J., Kent, A.J.R. & Tegner, C. 2021: The volatile and trace element composition of apatite in the Skaergaard intrusion, East Greenland. Contributions to Mineralogy and Petrology **176**, 102. *https://doi.org/10.1007/s00410-021-01861-x*

Salmonsen, L.P. & Tegner, C. 2013: Crystallisation sequence of the Upper Border Series of the Skaergaard Intrusion: revised subdivision and implications for chamber-scale magma homogeneity. Contributions to Mineralogy and Petrology **165**, 1155–1171. *https://doi.org/10.1007/s00410-013-0852-y*

Tegner, C. 1997: Iron in plagioclase as a monitor of the differentiation of the Skaergaard Intrusion. Contributions to Mineralogy and Petrology **128**, 45–51. *https://doi.org/10.1007/s004100050292*

Tegner, C., Andersen, T.B., Kjøll, H.J., Brown, E.L., Hagen-Peter, G., Corfu, F., Planke, S. & Torsvik, T.H. 2019: A mantle plume origin for the Scandinavian Dyke Complex: a piercing point for the 615 Ma plate reconstruction of Baltica. Geochemistry, Geophysics, Geosystems **20**, 1075–1094. *https://doi.org/10.1029/2018GC007941*

Tegner, C. & Cawthorn, R.G. 2010: Iron in plagioclase in the Bushveld and Skaergaard intrusions: implications for iron contents in evolving basic magmas. Contributions to Mineralogy and Petrology **159**, 719–730. *https://doi.org/10.1007/s00410-009-0450-1*

Tegner, C., Thy, P., Holness, M.B., Jakobsen, J.K. & Lesher, C.E. 2009: Differentiation and compaction in the Skaergaard Intrusion. Journal of Petrology **50**, 813–840. *https://doi.org/10.1093/petrology/egp020*

Thy, P., Tegner, C. & Lesher, C.E. 2009: The Skaergaard liquid line of descent revisited. Contributions to Mineralogy and Petrology **157**, 735–747. *https://doi.org/10.1007/s00410-008-0361-6*

Thy, P., Tegner, C. & Lesher, C.E. In press: Petrology of the Skaergaard Layered Series. GEUS Bulletin **56**, 8327. *https://doi.org/10.34196.v53.8327*

Wager, L.R. & Brown, G.M. 1968: Layered Igneous Rocks. 588 pp. Edinburgh and London: Oliver and Boyd.

Wager, L.R., Brown, G.M. & Wadsworth, W.J. 1960: Types of igneous cumulates. Journal of Petrology **1**, 73–85. *https://doi.org/10.1093/petrology/1.1.73*

Wager, L.R. & Deer, W.A. 1939: Geological investigations in East Greenland. Part III. The petrology of the Skaergaard Intrusion. Kangerdlussuaq, East Greenland. Meddelelser Om Grønland **105**, 352 pp.